Field-Oriented Control of an Induction Machine in a High Frequency Link Power System

SEUNG K. SUL, MEMBER, IEEE, AND THOMAS A. LIPO, FELLOW, IEEE

Abstract—**A field-oriented controlled induction machine drive operating with a high frequency single phase sinusoidal voltage link is presented. System performance is investigated by computer simulation and is verified by test on an actual prototype system. A novel control loop to minimize the link voltage fluctuation is proposed. The capability of rapid demagnetization of the induction machine by current regulation is investigated. A new current modulation technique, termed switch mode selection, is proposed and its performance is compared with the conventional delta modulation technique.**

INTRODUCTION

STATIC power converters for ac drives have traditionally employed a dc link as an interface between the fixed frequency power of the source and the variable frequency power of the load. The dc link is ideal for temporary energy storage since the energy storage can be easily accomplished at relatively low cost. However, the dc link has also several disadvantages. In particular, the hard switching of the power devices generates a high level of losses and device stresses which restricts the switching frequency to a few kHz, at most, when the power exceeds several tens of kilowatts. The lower switching frequency results in poorer system response and reduced power densities. A switching frequency of a few kHz also results in troublesome audible and electrical noise.

Power density considerations are a particularly important aspect of avionic and space systems. In general, avionic systems use 400 Hz as the distribution frequency because of its higher power density compared to commercial 60/50 Hz. However, recent work has suggested the use of a 20-kHz single phase ac for avionic and space station power distribution [1], [2]. Also, a new power converter topology and modulation technique to synthesize low frequency voltage and current from a 20-kHz link has been reported [3], [4]. These new systems offer the potential for greatly improved power density by reducing the size of bulky transformers and by decreasing the heat sink requirements of the power converters.

In this paper a complete electro-mechanical energy conversion system operating with a high frequency link is investigated. The induction machine is selected as the electromechanical energy converter because of its ruggedness, low cost and capability for rapid demagnetization. The last point, demagnetization, is particularly important in the space station application, where rapid replacement or rewind is not practical and where reliability is a particular concern. In such an application the rotating magnetic field within the machine must be extinguished upon experiencing an internal fault. The induction machine is ideally suited to this requirement since the machine inherently looses excitation when the terminal voltages are reduced to zero.

In order to provide good torque control over a wide speed range, a field-oriented control is typically embedded in the system. Instantaneous current regulation with indirect field-oriented control also permits faster response for demagnetization and protection from over-current conditions. The performance of field oriented control systems using instantaneous current regulation greatly depends on how accurately the actual machine current follows its reference. In conventional dc link systems the delta modulation technique is frequently used [5]. The delta modulation method has also been modified for use in zero voltage switching converters [3], [4]. This control method, also termed area comparison pulsewidth modulation, uses the integral of the error to operate a comparator which, in turn, performs the appropriate switching of the converter switches. When current rather than voltage is the regulated variable, the integration function is inherently performed by the load inductance and the explicit integrator can be eliminated [6], [7]. When the ratio between the switching frequency and the synthesized output frequency is large or when the load inductance is sufficiently great, delta modulation is sufficient to guarantee good performance of the field oriented control. However, in other cases, for example when driving a low inductance 400-Hz induction machine, the performance of the delta modulator is not sufficient to guarantee good current regulation. In this paper, a new current modulation technique for zero voltage switching type converters which substantially improves the frequency response of the high frequency link converter is proposed and verified by experiment [8].

20-kHz SINGLE PHASE SOURCE

In an orbiting space station or avionic application, energy is typically stored in dc form so that one side of the 20-kHz link must be interfaced to a dc source. Hence, the

Manuscript received February 16, 1988; revised March 26, 1990. This paper was presented at the 1988 IEEE Power Electronics Specialists Conference, Kyoto, Japan, April 11-14.

The authors are with the University of Wisconsin, Department of Electrical and Computer Engineering, 1415 Johnson Drive, Madison, WI 53706-1691.

IEEE Log Number 9037438.

0885-8993/90/1000-0436$01.00 © 1990 IEEE

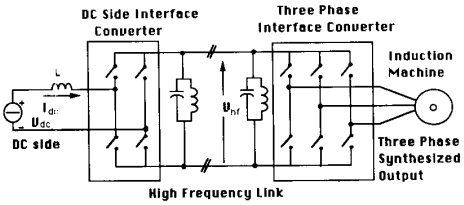

Fig. 1. Schematic of ac resonant voltage link system utilizing two interface converters and two parallel resonant tank circuits.

20-kHz link energy must initially be obtained from the dc source. There are several means to establish a 20-kHz single phase voltage bus from a dc source. The most well known method is to utilize a parallel output series resonant (POSR) converter [9], [10]. In this system the output frequency can be accurately maintained regardless of slight variations of the parameters of the resonant tank circuit. The output voltage can be regulated automatically within the expected range of the load variation. However, due to the high frequency switching in the presence of high voltage, the switching loss is considerable. Also, substantial ac current circulates on the dc side. This additional current increases the stresses of all power semiconductors in the POSR converter.

Another possibility for converting dc power to 20 kHz is to utilize a single phase converter which has same topology as the converter used to synthesize three phase, low frequency from the 20-kHz link. Because the converter has a capability of bi-directional power flow, the 20-kHz link voltage link can be energized in controlled fashion by transfer of power from the dc side to the resonant tank.

The overall system under consideration in this paper is shown in Fig. 1. Note that each interface converter is equipped with a resonant tank. The series inductance in the high frequency link is the equivalent inductance of the 20-kHz link distribution line. Each switch is assumed to have bi-directional current flow and voltage blocking capability.

Since the circuit is resonant, the ac link voltage must be regulated by means of a voltage regulator. The link voltage can be readily controlled by adjusting the dc side current, that is by regulating the power fed to the link tank circuit. The problem of link voltage regulation is addressed in another portion of this paper. It is clear that the link frequency is solely determined by the parameters of the tank circuit. A computer simulation illustrating voltage build-up and regulation of the ac link is shown in Fig. 2. The parameters of the link and converter are L_o = 22.5 μh, C_o = 3 μf, L = 3 mh, V_{dc} = 115 V. Losses of the inductors are also included.

Field-Oriented Control

To demonstrate the feasibility of field oriented control with a 20-kHz sinusoidal high frequency link, the system shown in Fig. 3 has been simulated. In this simulation, the high frequency link is assumed to function as an ideal

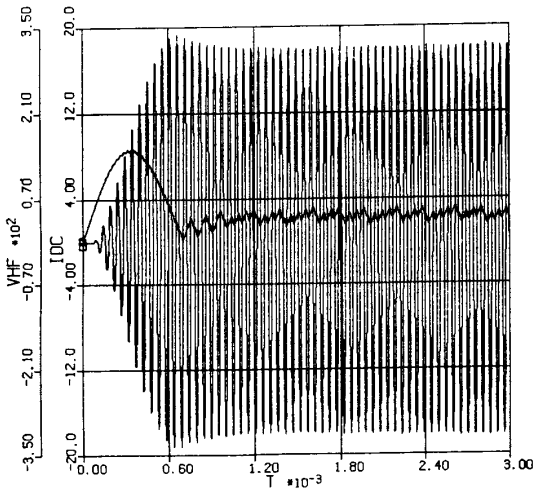

Fig. 2. Simulation results of high frequency link voltage build-up and regulation with three phase interface converter disabled. Traces show converter dc side input current in amperes and link voltage in volts.

voltage source. Hence, the LC tank circuit and the effects of power flow to the resonant link are neglected. Typical starting and load torque transient responses are shown in Fig. 4(a) and (b). It should be noted that the machine side current synthesized from the high frequency link voltage is nearly sinusoidal and varies exactly according to the torque variations. The torque and speed responses also demonstrate very good performance.

One important aspect of the circuit behavior is the response of the input power entering the interface converter. It can be noted that the instantaneous power at this point varies very widely and even changes its polarity although its filtered or moving average value indicates no negative values. Because the converter is switched according to the error between the reference current and actual current, it is clear that the power may be negative during a certain switching instant even though the average power remains positive.

The response of demagnetization control is shown in Fig. 5. Demagnetization of the induction machine is achieved within a few cycles after the command is initiated without presence voltage spikes. For all of the above simulations the parameters of a 3-hp 4-pole 60-Hz induction machine has been used.

Voltage Regulation

It is clear that the instantaneous power variation mentioned in the previous section will result in a link voltage fluctuation unless the variation in power is matched perfectly by the other converter and source on the same link. However, the number of switching modes of the dc side interface converter is only three while that of the machine side interface converter is seven. Moreover, the rate at which the dc source power can change is determined by the dc source voltage, high frequency link voltage, and dc source filter inductance. Hence, power matching con-

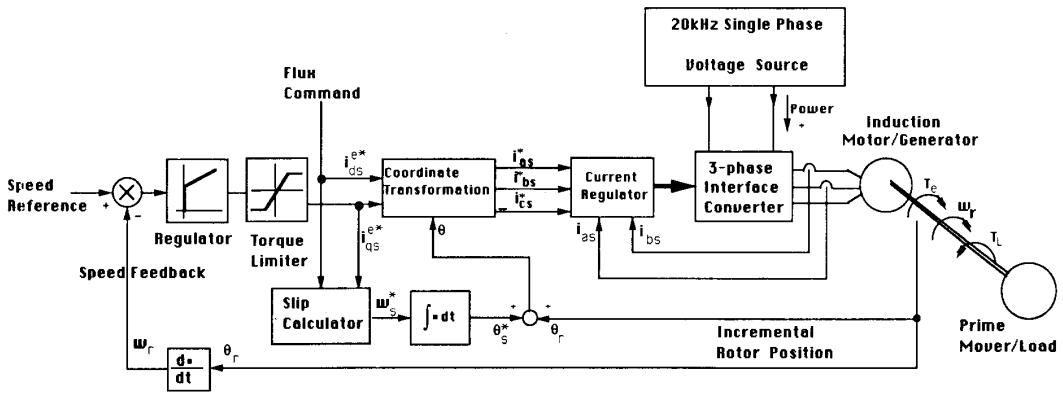

Fig. 3. Control block diagram of field-oriented controlled induction machine drive system utilizing high frequency source.

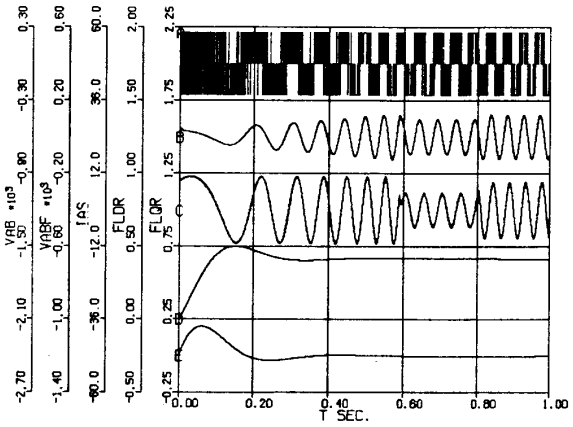

(a)

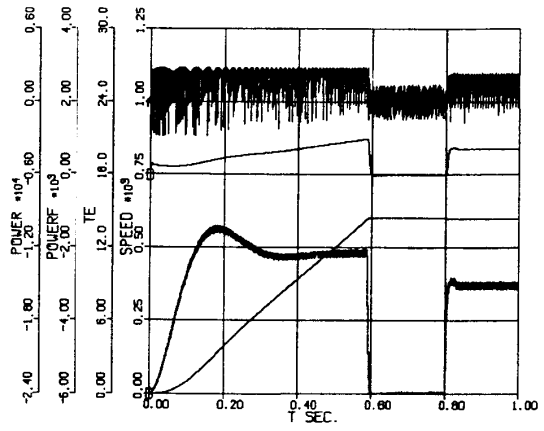

(b)

Fig. 4. (a) Response of system Fig. 3 during starting and with load torque transient. Traces: line voltage and filtered line voltage in volts, line current in amperes, rotor flux d- and q-axis components in webers in synchronously rotating reference frame. (b) Response of system of Fig. 3 during starting and with load torque transient. Traces: 1) input power to interface converter, 2) filtered input power in watts, 3) machine torque in nt-m, 4) speed in r/min and 5) slip angular velocity in rad/s.

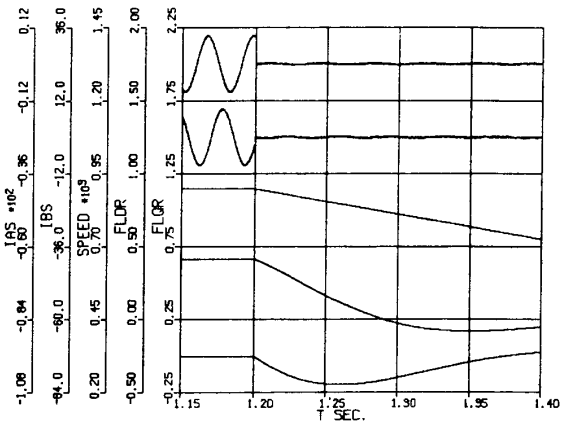

Fig. 5. Response of system of Fig. 3 during rapid demagnetization. Traces: A phase and B phase line current in amperes, speed in r/min, rotor flux d- and q-axis components in webers.

trol on an instantaneous basis does not appear to be possible. At best, with an ideal controller, average power matching can be achieved. Hence, the ripple power must be handled by the tank circuit at the cost of link voltage variation. With an well designed average power matching controller, however, the link voltage variation can be minimized.

The simplest approach for obtaining average power information is to measure the power supplied to the induction machine and use a low pass filter, as shown in Fig. 6. However, with this method time delays resulting from the lower pass filter are inevitable. Thus, during the delay time the difference between the average and instantaneous power must be covered by the power capability of the tank circuit. This observation, in turn, implies a degradation in the link voltage regulation. To lessen this problem, a voltage regulation loop which generates a current reference from the link voltage error can be added to the power matching loop as a minor loop. The simulation results of this controller are shown in Fig. 7(a) and (b).

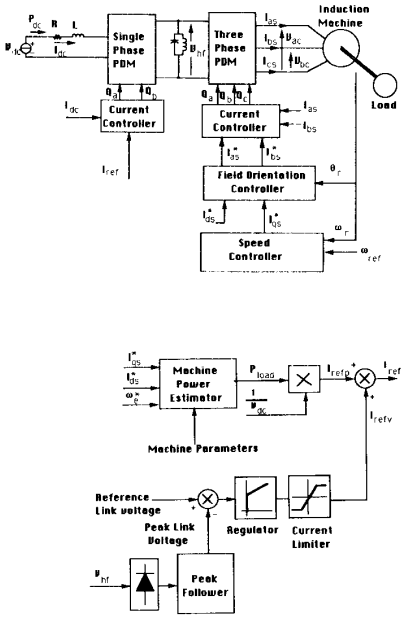

Fig. 6. System control block diagram and controller utilizing power measurement as major loop and minor loop voltage regulation.

Another method to obtain an average power signal is to estimate the power with information derived from the reference currents of the induction machine which are, in turn, available from the field oriented control algorithm used to control the induction machine [9]. If the current regulation is perfect and if the machine parameters do not change and are known, the average machine power can be estimated without any time delay. In practice, of course, there are always differences between the actual currents and their references. Moreover, the parameters of the machine change according to flux level and operating temperature so that some error between estimated power and the actual power is inevitable. However, these errors can be compensated by using a voltage regulating loop as a minor loop as in the previous method. The block diagram of this controller is shown in Fig. 8 and the corresponding simulation results are given in Fig. 9(a) and (b).

In this simulation the value of power which is used for average power matching is 90% of the exact value. In order to allow for an error in the estimation, an intentional 10% estimation error is made. From Fig. 9(a), it can be observed that the torque and speed responses are nearly the same as using actual power measurement. For the purpose of evaluating the regulation capability of the various controllers it is useful to define the error criterion:

$$\text{criterion} = \int_0^T (V_{\text{ref}} - V_{\text{hfpeak}})^2 \, dt,$$

where T is the simulation interval.

The criterion value of the previous power measurement controller is 222 while the result using power estimation

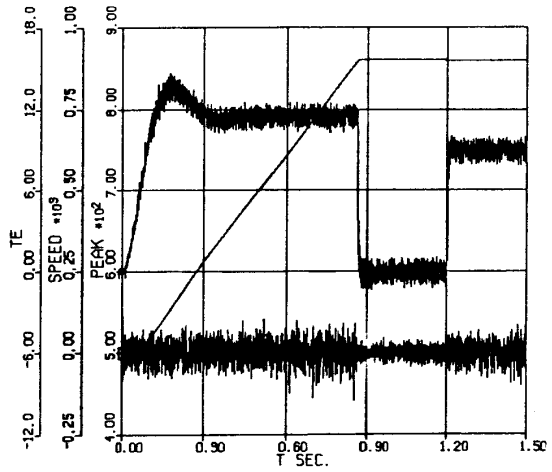

(a)

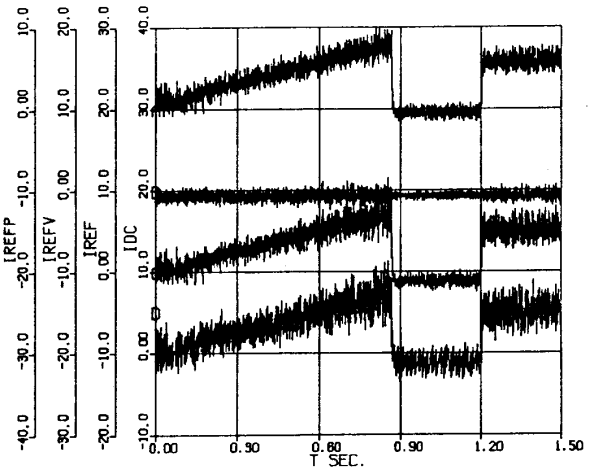

(b)

Fig. 7. (a) Transient response of voltage controller of Fig. 6. Traces: 1) Electromagnetic torque in nt-m, 2) speed in rpm, and 3) peak voltage of the high frequency link in volts. (b) Transient response of voltage controller of Fig. 6. Traces show: component of reference current for power matching in amperes, component of reference current for voltage regulation in amperes, reference current in amperes, and dc source current in amperes.

from the field-oriented controller is 190. Hence, the regulation of this controller is better in spite of the 10% estimation error. Note that the component of the reference current for average power matching shown in Fig. 9(b) contains no ripples since it is derived from the estimated power. The component derived from the minor voltage regulation loop shows some ripple. However, the ripple in the reference current is smaller than that of previous case. Therefore, the ripple in the actual dc source current is less severe. In the actual implementation, reduced ripple in the actual current has many advantages such as lower losses in power components, lower current rating of power components and easier protection of system. It

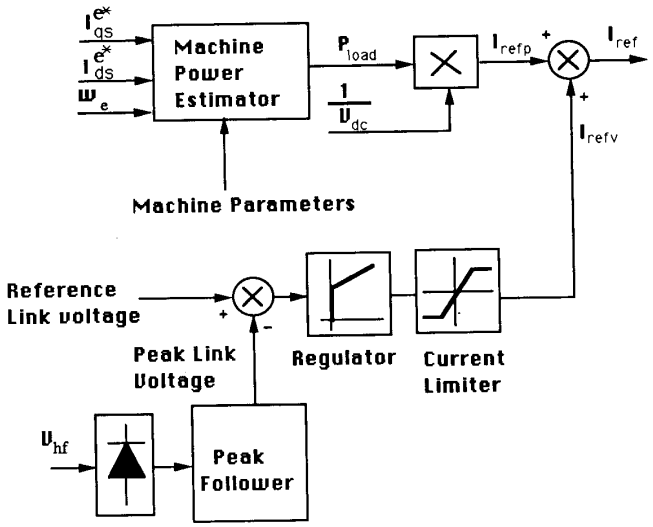

Fig. 8. Controller block diagram utilizing power estimation and supplementary link voltage regulation.

is also important to mention that in addition to its superior response, the power estimation method is also easier to implement since it requires no additional power measurement.

Optimal Current Regulation

It is well-known that regulation of the induction machine side current is crucial for satisfactory performance of a field oriented control system. If the ratio between switching frequency and output frequency is large, or if the load inductance is substantial, then the simple delta modulator is sufficient to obtain reasonable performance. However, in aerospace applications, control of a 400-Hz induction machine is frequently required. Fig. 10 depicts a new switch mode selection controller which is specifically designed to obtain optimum performance from a high frequency link. The controller operates on a principle which recognizes that in almost every kind of resonant converter using a zero voltage or zero current switching scheme the switching instant and pulse duration is known in advance of the actual switching instant. Hence, the problem of current modulation reduces to finding the next optimal combination of switch states at the very switching instant which minimizes some specific error criterion. For this purpose the induction motor can be modeled as simply a voltage behind transient reactance. Based on the present motor current state, the instantaneous time variation of the motor current which would occur at the next switching instant for all seven possible switch combinations can then be calculated in closed form. Since the load current for the next switching instant can be predicted for all possible switching states before the switching instance actually occurs, the switching pattern can then be selected which minimizes a specified error function. If current regulation only is required, the error function may be defined as simply the sum of the absolute current regulation errors of each phase or the sum of the square of the individual errors. The error function principles can be extended to any form which satisfies a specific requirement. For example, to obtain improved voltage regulation, it may be useful to also include a term which depends upon the instantaneous power variation.

Performance of the new switch mode selection controller compared to the delta modulator has been evaluated in detail by computer simulation. Typical results are shown in Figs. 11 and 12. In these simulations a 400-Hz 7.5-hp 4-pole induction machine was considered and the 20-kHz link again assumed as an ideal single phase voltage source. To compare the regulation following switching criterion has been calculated for each case:

$$\text{criterion} = \int_0^T \left[(i_{as} - i_{aref})^2 + (i_{bs} - i_{bref})^2 + (i_{cs} - i_{cref})\right]^2 dt.$$

The value of the criterion for delta modulation and for the switch mode selection controller corresponding to Figs. 11 and 12 are 0.2297 and 0.1081, respectively. Hence, it appears that the mode controller offers substantial improvements in current regulation over the delta modulator. The drawback of this controller is that it requires numerous mathematical operations which are difficult to accomplish in real time so that the controller becomes much more complex than other controllers.

Experimental Results

The high frequency link motor drive which was studied by means of simulation has also been constructed and tested in the laboratory. In particular, the complete system of Fig. 2 has been implemented together with an indirect field oriented controller (Fig. 3) voltage regulator

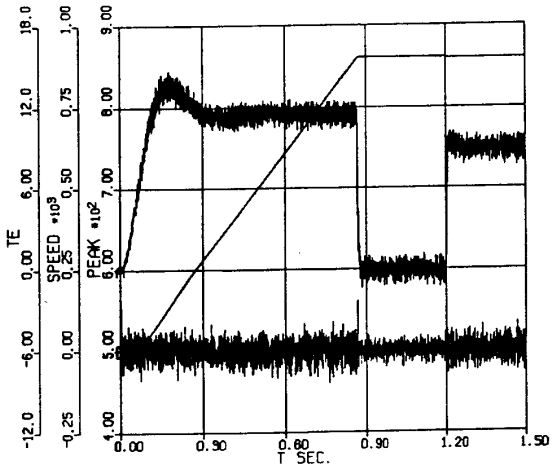

(a)

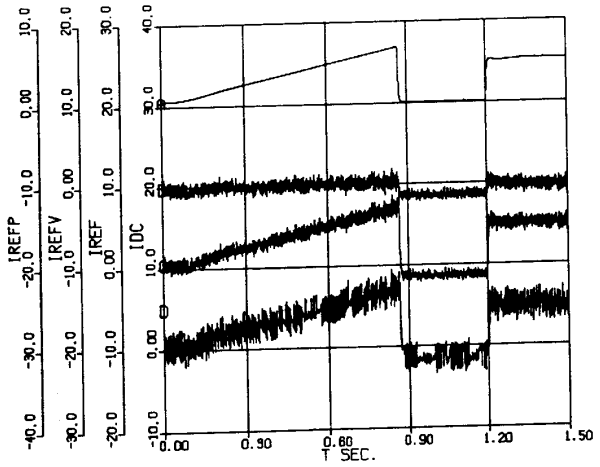

(b)

Fig. 9. (a) Response of voltage controller utilizing power estimator of Fig. 8. Traces: 1) electromagnetic torque in nt-m, 2) speed in r/min, and 3) peak voltage of high frequency link in volts. (b) Response of voltage controller employing power estimator of Fig. 8. Computer traces: component of reference current for power matching in amperes, component of reference current for voltage regulation in amperes, reference current in amperes, and dc source current in amperes.

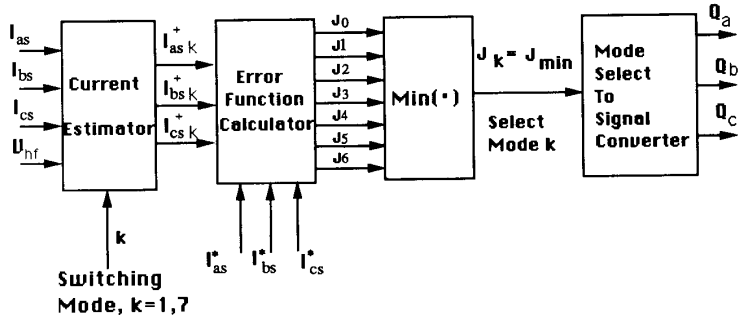

Fig. 10. Block diagram of switch mode selection controller for induction motor current regulation.

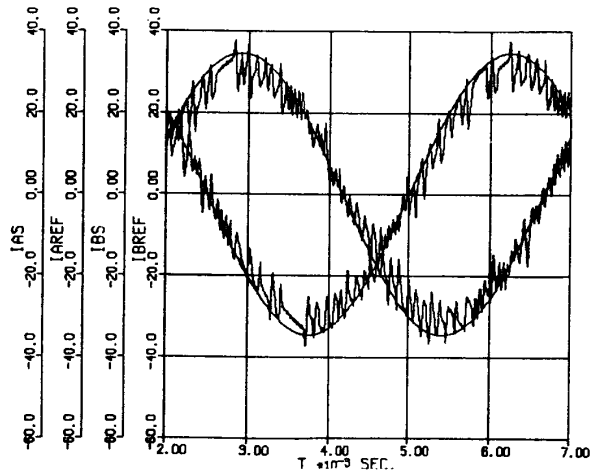

Fig. 11. Response of motor current regulator employing delta modulator. Traces: 1) A phase and 2) B phase line currents and reference currents in amperes.

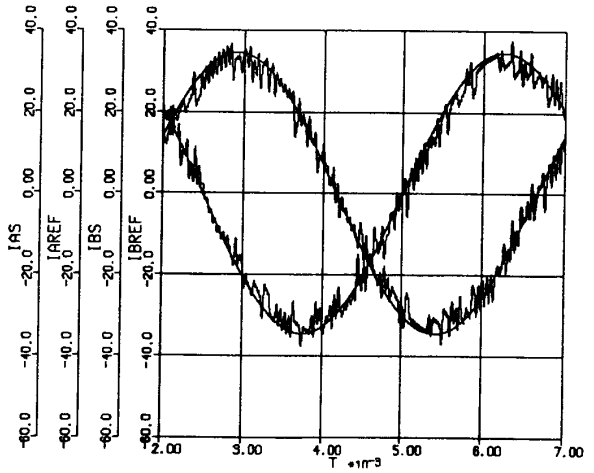

Fig. 12. Response of motor current regulator utilizing switch mode selection controller. Traces: 1) A phase and 2) B phase line currents and reference currents in amperes.

(Fig. 8) and switch mode selection current regulator (Fig. 10).

Voltage Build-up

. An experimental result obtained during controlled voltage build-up is shown in Fig. 13. A smooth, controlled build-up can be observed which agrees well with the simulation results shown in Fig. 2. It can be noted that during the steady-state, a current which supplies the losses of the system continues to flow from the dc source.

Dynamic Performance of Field-Oriented Control

Test results illustrating dynamic performance of the field oriented controller is shown in Fig. 14(a) and again

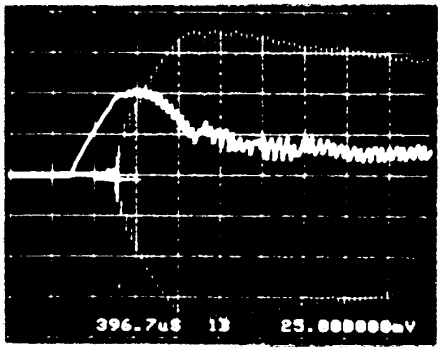

Fig. 13. Experimental waveforms of high frequency link voltage and dc source current during voltage build-up. Traces: high frequency link voltage: 120 V/div., dc source current; 5 A/div., time scale: 396.7 μs/div.

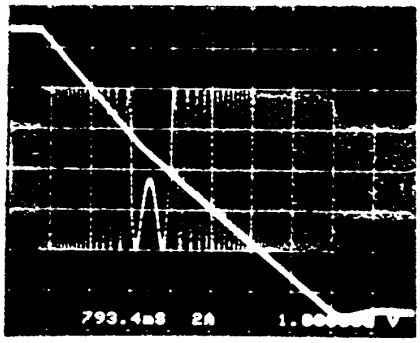

(a)

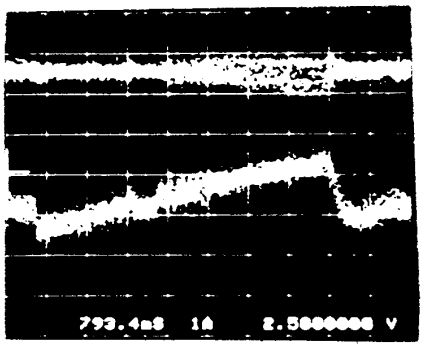

(b)

Fig. 14. (a) Performance of induction machine during speed reversal employing field-oriented controller. 1) Speed: 190 r/min/div., 2) A phase current: 5 A/div., time scale: 793.4 ms/div. (b) Additional Experimental waveforms corresponding to Fig. 14a. Top trace: peak voltage: 130 V/div., reference: 4 div. from bottom. Bottom trace: dc source current: 5 A/div., reference: 3 div. from bottom. Time scale: 793.4 ms/div.

appear similar to the simulation results except for the time scale. The difference in the time scale is mainly due to the difference of the inertia of the actual mechanical system. In the simulation a small inertia was utilized to save simulation time while in the actual drive, a 7.5-kW dc

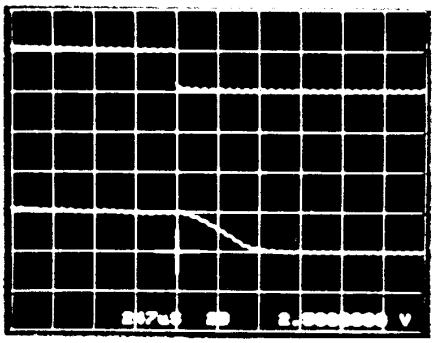

(a)

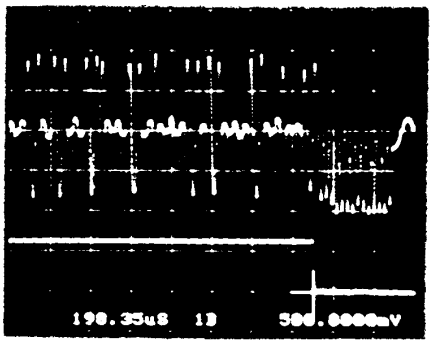

(b)

Fig. 15. (a) Measured waveforms during rapid demagnetization. Top trace: demagnetization command. Bottom trace: A phase induction machine current; Scale: 5 A/div., Time scale; 247 μs/div. (b) Additional experimental waveforms during rapid demagnetization Top trace: induction machine AB line to line voltage, scale: 200 V/div. Bottom trace: demagnetization command. Time scale: 198.35 μs/div.

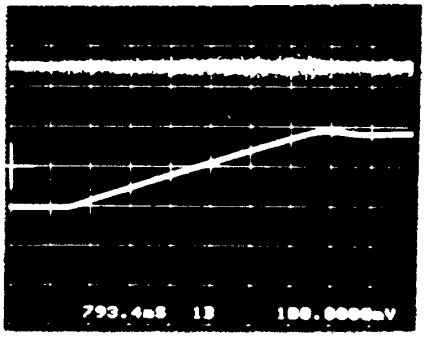

(a)

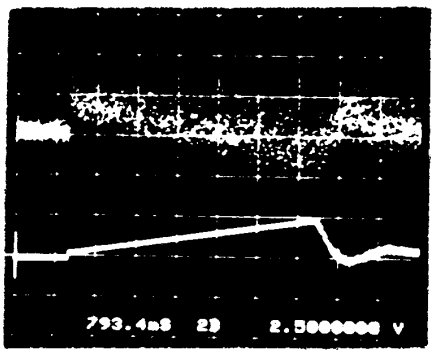

(b)

Fig. 16. (a) Performance of power estimation controller. Top trace: peak ac voltage, scale; 130 V/div. Reference is 4 div. from bottom. Bottom trace: induction motor mechanical speed; 190 r/min/div. Reference is 3 div. from bottom. Time scale: 793.4 ms/div. (b) Performance of power estimation controller. Top trace: dc source current reference from voltage controller (I_{ref_V}), scale: 1.5 A/div. Zero reference 5 div. from the bottom. Bottom trace: reference current from power estimator (I_{ref_P}); scale: 5 A/div. Reference is 2 div. from bottom. Time scale: 793.4 ms/div.

machine and pulley was coupled to the induction machine. Also in the experiment, differences in deceleration and acceleration time can be attributed to variations of the friction constant of the dc machine which depends on the direction of rotation. The trace of the A phase current clearly indicates good current regulation. In this test the delta modulator is used as the current regulator. In Fig. 14(b) waveforms corresponding to the dc side current and the peak of the high frequency link voltage are shown. Note that the dc current varies according to the mechanical power to continually produce a power balance. The trace corresponding to the peak of the link voltage shows reasonably good voltage regulation.

Demagnetization

The waveform for the A phase induction machine current during demagnetization is shown in Fig. 15. Note that the current is brought to zero within 500 μs. The line to line voltage at the command remains negative to decrease the current. The figures clearly demonstrate very fast extinction of the machine current without appearance of voltage spikes (i.e., high di/dt) across the motor terminals.

Power Estimation Controller

The behavior of the power estimation controller is shown in Fig. 16. With the starting of the induction machine the reference current from estimated power gradually increases and, after settling of the speed, the current decreases to the small value needed to supply the losses of the system. The reference current from the voltage regulator, which is a minor loop, deviates around zero suggesting that this regulator is performing only a small corrective action. By comparing the magnitude of the current it can be noted that the major part of the dc source reference current is derived from the power estimator. The experimental results shows good agreement with the simulation results which were portrayed in Fig. 9.

Current Regulation

The current regulation capability of the delta modulator is demonstrated in Fig. 17. In this case a 13-Hz ac current is synthesized with 3-hp 60-Hz pole induction machine load. It is apparent that the result is already nearly ideal so that if the switch mode selection controller were used

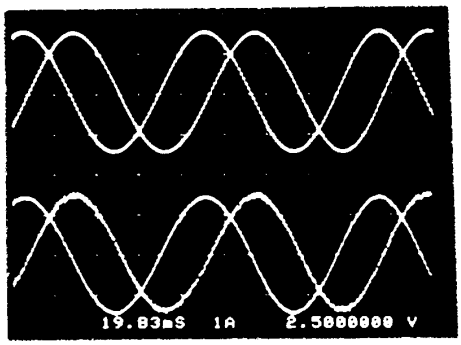

Fig. 17. Synthesis of 13-Hz motor stator currents using delta modulation. Top trace: A and B phase reference current, scale: 5 A/div. Bottom trace: Corresponding measured motor current, scale: 5 A/div. Time scale: 19.83 ms/div.

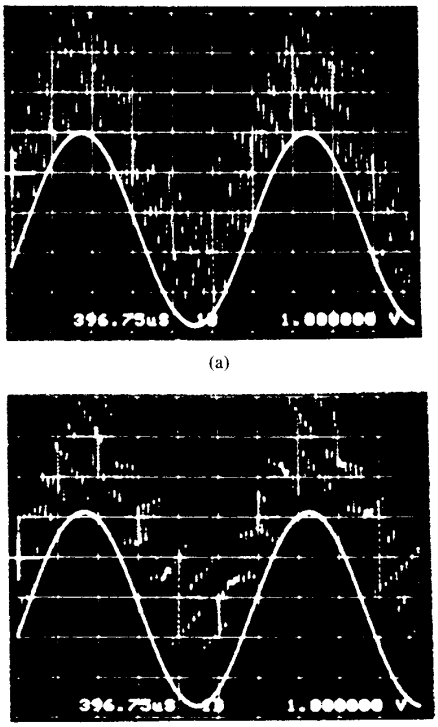

(a)

(b)

Fig. 18. (a) Current waveform synthesis of 450-Hz motor currents showing A phase actual current and corresponding reference using delta modulation. Magnitude: 2.5 A/div. Time scale: 396.75 μs/div. (b) Current waveform synthesis of 450 Hz motor currents showing A phase actual current and corresponding reference using switch mode selection controller. Magnitude: 2.5 A/div. Time scale: 396.75 μs/div.

there would be no detectable difference. In order to better compare the delta modulator and the switch mode controller a 1 mH 3 phase, *Y* connected inductor load was used in place of the induction motor and a 450-Hz current waveform synthesized from the 20-Hz link. The results for the two current controllers are shown in Fig. 18. It is clear from the figures that the switch mode selection controller shows smaller ripple content and therefore improved tracking of the current command.

Conclusion

In this study the use of field oriented induction motor control with a high frequency resonant link system has been demonstrated. The following results have been obtained.

1) Current regulated field oriented controllers can be successfully applied to high frequency link induction machine drive systems. The response of the system is comparable or even exceeds more conventional current regulated PWM systems.

2) The excitation field of the induction machine can be readily eliminated within a few cycles by simply commanding the reference current to zero. The feature has important implications in avionic and space applications.

3) By use of power estimation control, high frequency ac link voltage fluctuations can be substantially reduced thereby reducing voltage blocking requirements of the converter switches.

4) Utilization of switch mode selection control for the synthesis of ac current indicates that substantial improvement in the current regulation capability is possible compared to simple delta modulation when synthesizing high frequency waveforms.

Acknowledgment

The work reported in this paper was sponsored by the NASA Lewis Research Center, Cleveland, OH under contract NAG 3-786.

References

[1] I. G. Hansen and G. R. Sundberg, "Space station 20 kHz power management and distribution system," in *1986 Power Electronics Specialist's Conf. Rec.*, Vancouver, Canada, June 1986, pp. 676-683.

[2] A. C. Hoffman, I. G. Hansen, R. F. Beach, *et al.*, "Advanced secondary power system for transport aircraft," NASA Technical Paper 2463, 1985.

[3] P. K. Sood and T. A. Lipo, "Power conversion distribution system using a resonant high-frequency ac link," in *Conf. Rec. 1986 Annu. Meet. Ind. Appl. Soc.*, pp. 533-541.

[4] P. Sood, T. A. Lipo, and I. Hansen, "A versatile power converter for high frequency link systems," in *1987 Applied Power Electronics Conf. Rec.*, March 2-6, 1987, San Diego, CA.

[5] P. Ziogas, "The delta modulation technique in static PWM inverters," *IEEE Trans. Ind. Appl.*, vol. IA-17, pp. 199-204, Apr. 1981.

[6] M. Kheraluwala and D. M. Divan, "Delta modulation strategies for resonant link inverters," in *1987 IEEE Power Electronics Specialists Conf. Rec.*, Blacksburg, VA, pp. 271-278.

[7] R. D. Lorenz and D. M. Divan, "Dynamic analysis and experimental evaluation of delta modulators for field oriented ac machine current regulation," in *Conf. Rec. 1987 Annu. Meet. IEEE Ind. Appl. Soc.*, pp. 196-201.

[8] S. K. Sul and T. A. Lipo, "Design and test of bi-directional speed and torque control of induction machines operating from high frequency link converter," NASA report, Contract No. NAG 3-786, Mar. 1988.

[9] N. Mapham, "An SCR inverter with good regulation and sine-wave output," *IEEE Trans. Ind. Gen. Appl.*, vol. IGA-3, pp. 176-187, Mar./Apr. 1967.

[10] T. A. Lipo and P. K. Sood, "Study of the Generator/Motor Operation of Induction Machine in a High Frequency link Space Power System," NASA Report, Contract No. NAG-3-631, Sept. 1986.

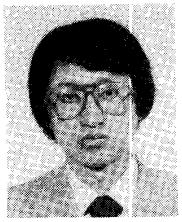

Seung Ki Sul (S'78-M'87) was born in Pusan, Korea on March, 1958. He received the B.S., M.S., and Ph.D. degrees from Seoul National University, Seoul, Korea, in 1980, 1983, and 1986, respectively.

He was a Visiting Research Associate at the University of Wisconsin-Madison from 1986 to 1988. He is now with GoldStar Industrial Systems Co. in Seoul, Korea as a Principal Research Engineer.

His current research interests are in high frequency resonant inverter for high power applications and digital signal processing of machine drive systems.

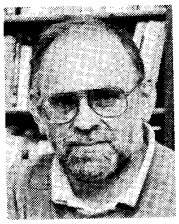

Thomas A. Lipo (M'64-SM'71-F'87) received the B.E.E. and M.S.E.E. degrees from Marquette University, Milwaukee, WI, and the Ph.D. degree in electrical engineering from the University of Wisconsin-Madison, in 1962, 1964, and 1968, respectively.

From 1969 to 1979 he was an Electrical Engineer in the Power Electronics Laboratory of Corporate Research and Development of the General Electric Company, Schenectady, NY. In 1979 he became Professor of Electrical Engineering at Purdue University, Lafayette, IN. He joined the faculty of the University of Wisconsin in 1981, where he is presently a Professor of Electrical Engineering.

He has maintained a deep interest in power electronics and ac drives for over 25 years. Dr. Lipo holds ten patents, has published over 100 papers and has received 11 prize paper awards. He is an active member of five IEEE Committee or Subcommittees and is past Chairman of two of them. He is also a member of the Executive Board of the Industry Application Society.